Evaluation of factors affecting pyrite oxidation and subsequent pollutant generation in backfilled open cut coal mines

R. N. Singh

Professor of Mining Engineering, Faculty of Engineering, University of Wollongong

Northfields Avenue, Wollongong, NSW 2522, Australia.

E-mail: raghu@uow.edu.au

F. Doulati Ardejani

Lecturer, Faculty of Mining, Shahrood University of Technology, Iran

E-mail: fdoulati@shahrood.ac.ir

ABSTRACT

The oxidation of iron sulphide minerals, especially pyrite, by oxygen and water in the presence of certain bacteria causes acid mine drainage (AMD), with high concentrations of iron and sulphate and low pH. The results of a numerical finite volume simulation of AMD generation at abandoned backfilled open cut mines are presented. The governing equations of pyrite oxidation, oxygen diffusion and solute transport have been solved by modifying a commercial computational fluid dynamics package called PHOENICS. The pyrite oxidation rate is described by a shrinking-core model for spherical pyritic grains. Oxygen transport within the backfill material is assumed to be by diffusion. A sensitivity analysis of the major parameters that influence the rate of the pyrite oxidation and subsequent pollutant generation has been carried out. The parameters considered were the effective diffusion coefficient for oxygen transport, the surface recharge rate, the radius of spoil particles containing pyrite, the pyrite content, and the role of bacteria on the pyrite oxidation rate. It was found that the pyrite oxidation rate and the subsequent pollutant loading are most sensitive to the effective diffusion coefficient in the presence of iron-oxidising bacteria, although the effect of the particle radius should not be ignored. An increasing diffusion coefficient for oxygen transport increased the rate of pyrite oxidation and subsequently increased the ferrous iron and sulphate concentrations and decreased the solution pH. Iron-oxidising bacteria increased the ferric/ferrous ratio. The bacterially mediated oxidation of pyrite is highly dependent on the pH. When the pH is maintained in the range between 2.5 to 3.5, the bacterial oxidation of pyrite is enhanced. Subsequently, the bacterial action produces more Fe^{3+}, SO_4^{2-}, H^+, and Fe^{2+}. The results of such sensitivity analyses are important in assessing and evaluating the physical and chemical processes involved in the generation of pollutants and the transport of dissolved chemical species from an open cut mine into an aquifer.

INTRODUCTION

One of the most important features in the simulation of long-term pyrite oxidation and pollutant generation in an open cut mine is the predicted variability when the values of the modelling parameters are changed. According to Jaynes et al. (1984b), changes in any of the important parameters can change the predicted rate of pyrite oxidation. In addition, the mutual dependence of the model parameters should not be ignored. Davis (1983) noted that a sensitivity analysis is required to improve insight into which model parameters govern predicted aspects such as pyrite oxidation and subsequent pollutant generation rate.

Quantifying the effect of variations in the model parameters on output quantities is also essential when we may wish to reduce a parameter, such as the sulphate production rate, below a prescribed level in order to minimise the pollution load on the receiving environs of a mine site. Alternatively, acceleration of the oxidation rate and the process of pollution production may also be desirable in order to decrease the reactive lifetime of the spoil and thereby reduce the duration of active monitoring at the mine site.

To consider the response of the model to changes in the parameter values used for modeling, the sensitivity of the model to changes in the effective diffusion coefficient for oxygen transport, the particle size, the pyrite content, the surface recharge rate and the role of iron-oxidising bacteria on the pyrite oxidation rate were all examined. In order to perform this sensitivity analysis, a numerical finite volume model has been developed by modifying a commercial computational fluid dynamics (CFD) package called PHOENICS. The necessary coding for additional source and sink terms and boundary conditions was written in the FORTRAN 99 language and was supplied in PHOENICS. These codings for all non-standard calculations were used in PHOENICS during the course of the solution process. The model was calibrated by comparison of the results produced by the present model with results obtained from the POLS numerical finite difference model developed by Jaynes et al. (1984a, b).

MATHEMATICAL EXPRESSIONS

In an earlier paper (Doulati Ardejani et al., 2002), the authors described a numerical model for prediction of long-term pyrite oxidation and subsequent pollutant production associated with open cut coal mines. The activity model developed by Jaynes et al. (1984a) was used after supplying FORTRAN coding in the user-accessible GROUND subroutine of the PHOENICS software in order to incorporate the role of iron-oxidising bacteria. A well known core-shrinking approach (Levenspiel, 1972) and a gaseous diffusion balance were used to describe pyrite oxidation and oxygen transport processes within the pore space of the spoil. The aqueous solutes were transported through the porous medium by the processes of advection and diffusion. The relevant equations are given below:

Pyrite oxidation equation:
$$\frac{\partial X}{\partial t} = \frac{-3 X^{\frac{2}{3}}}{6 \tau_{D_{[Oxd]}} X^{\frac{1}{3}} \left(1 - X^{\frac{1}{3}}\right) + \tau_{C_{[Oxd]}}} \tag{1}$$

Oxygen balance:
$$\phi_a \frac{\partial u}{\partial t} = D_e \left(\frac{\partial^2 u}{\partial x_j^2} \right) - S_{O_2} \tag{2}$$

Transport equation:
$$\phi \frac{\partial C_i}{\partial t} + \rho_b \frac{\partial \overline{C}_i}{\partial t} = D \frac{\partial^2 C_i}{\partial x_j^2} - q_j \frac{\partial C_i}{\partial x_j} \pm S , \ i = 1, 2, ..., N \tag{3}$$

where: X = the fraction of pyrite remaining within the particle (*kg/kg*); t = time (*s*); Oxd = oxidant; τ_C = time required for full oxidation of pyrite within a particle if the oxidation process is only controlled by the decreasing surface area of pyrite (*s*); τ_D = time required for full oxidation of pyrite within a particle when the oxidation rate is solely controlled by oxidant diffusion into the particles (*s*); ϕ_a = air-filled porosity of the spoil (m^3/m^3); u = oxygen in the spoil pore space (mol/m^3); D_e = effective diffusion coefficient (*m^2/s*); S_{O_2} = volumetric oxygen consumption as discussed in Jaynes et al. (1984a) and modified by Doulati Ardejani et al. (2002) (mol/m^3); C_i = dissolved concentration (mol/m^3); x_j = Cartesian coordinates (m); $\overline{C}_i$ = concentration in adsorbed form (*mol/kg*); ρ_b = bulk density of the medium (kg/m^3); S = sink and source terms representing the changes in aqueous component concentrations due to the chemical reactions; q_j = vector components of the pore fluid specific discharge (m/s); D = hydrodynamic dispersion coefficient (*m^2/s*); and N = number of the aqueous components. The expressions for τ_D and τ_C can be found in the literature (Levenspiel, 1972; Jaynes et al., 1984a; Doulati Ardejani et al., 2002).

MODELLING PERFORMANCE

A one-dimensional spoil profile with a depth of 10 m was divided into 20 0.5 m thick control volumes. The number of time steps used was 100. A total iteration of 1200 was assigned to the simulation. The y-direction was used to simulate vertical flow. It was assumed that the flow system was saturated and the water flow was steady state. The governing equations for the model were solved using Version 3.2 of the PHOENICS fluid dynamics software (Spalding, 1981; CHAM, 2000). The model input data were taken from Jaynes et al (1984b) and given in the author's earlier paper (Doulati Ardejani et al., 2002). The surface of the spoil was specified as a first type boundary condition with the oxygen concentration equal to the atmospheric concentration, 0.21 mole fraction. At the base of the spoil column, a zero-gradient boundary condition was assigned. It was further assumed that no oxygen initially existed within the profile. The spoil temperature was 15°C. For solute transport, the spoil surface was assigned a constant recharge of 0.5 m/yr. A hydrodynamic dispersion of 1.0x10^{-10} m^2/s was used to achieve consistency with the POLS model results. A first-type boundary condition was selected at the top surface of the spoil for the concentration of the oxidation products. An initial boundary condition was specified to describe the distribution of the dissolved ions within the water in the spoil profile. A zero-concentration gradient boundary condition was assumed at the outlet of the profile.

MODELLING RESULTS

Variations in any of the model parameters affect the rate of pyrite oxidation and subsequent pollutant generation. Sensitivity analyses of the major parameters that influence the rate of pyrite oxidation have been carried out by performing several simulations. The main parameters considered in this paper are the effective diffusion coefficient of oxygen transport, the role of iron-oxidising bacteria, the radius of the spoil particles containing pyrite, the surface recharge rate, and the pyrite content.

THE EFFECT OF OXYGEN DIFFUSION

The first simulation was performed to assess the sensitivity of the model to changes in oxygen diffusion. The effective diffusion coefficients ranged from a low value (1×10^{-8} m^2/s) to a high value representing well-drained spoil conditions (1×10^{-6} m^2/s) (Figure 1). Under the low diffusion value (1×10^{-8} m^2/s), oxygen penetrated less than 3 m in 5 years, compared with the well-drained spoil condition where the oxygen diffused over the entire spoil profile over the same time period.

As Figure 1 shows, the accuracy of the finite volume model (solid line) for the oxygen concentration was evaluated and verified by comparison with the results of the POLS finite difference model (Jaynes et al., 1984b), shown as dots for a diffusion coefficient of 1×10^{-7} m^2/s. The agreement was close.

Figure 2 shows the sensitivity of the pyrite oxidation rate (illustrated as fraction of the pyrite oxidised) to oxygen diffusion. This shows that the overall oxidation rate greatly depends on the effective diffusion coefficient. Increasing the effective diffusion coefficient significantly increased the amount of pyrite oxidation. For well-drained spoil conditions with an effective diffusion coefficient of 1×10^{-6} m^2/s, about 40% of the pyrite was consumed after 10000 days, while with a diffusion value of 1×10^{-8} m^2/s, the oxidised pyrite was less than 10%.

Figures 3 and 4 show the ferrous iron concentration and the solution pH versus time predicted at the discharge boundary of the model for different values of effective diffusion coefficients. Figure 3 shows that the maximum Fe^{2+} leaching rate occurred about 2100 days after the oxidation began and that it then reduced gradually over time. For a diffusion coefficient of 1×10^{-8} m^2/s, the peak concentration of Fe^{2+} was 1 mol/m^3 and it increased to 12.7 mol/m^3 when the effective diffusion coefficient increased to 1×10^{-6} m^2/s.

The pH dropped to its minimum value at 2100 days and then increased slightly over a period of time as illustrated in Figure 4. For a diffusion coefficient of 1×10^{-8} m^2/s, the pH never dropped below 2.6 at any point of the spoil profile. When the effective diffusion coefficient increased to 1×10^{-6} m^2/s, pH decreased to 1.6 at 2100 days and gradually increased to 2.05 at 10000 days of the reaction. Increasing the effective diffusion coefficient increased the rate of ferrous iron production and decreased the solution pH.
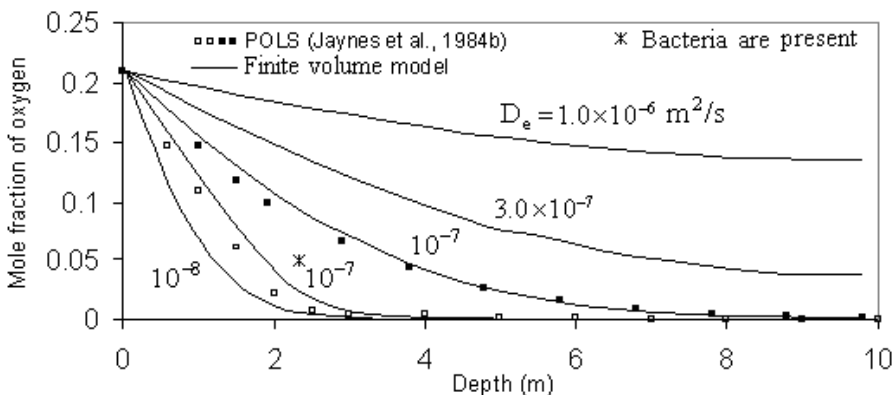

Figure 1. Oxygen mole fraction vs. depth after 5 years of simulation for different effective diffusion coefficients
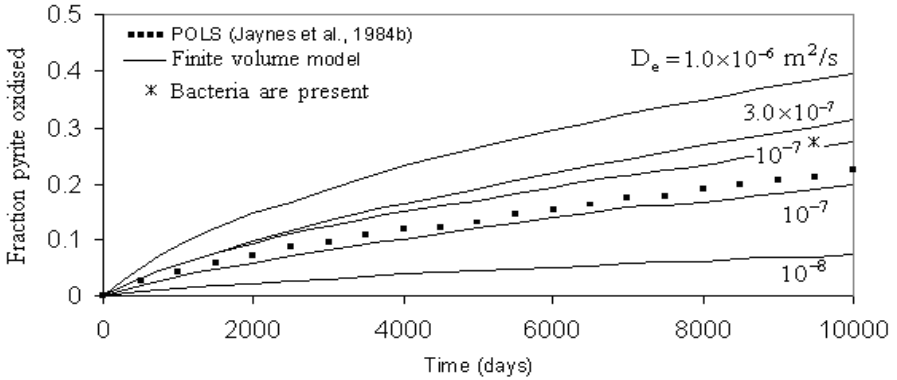
Figure 2. Pyrite fraction oxidised vs. time over entire spoil column for different effective diffusion coefficients
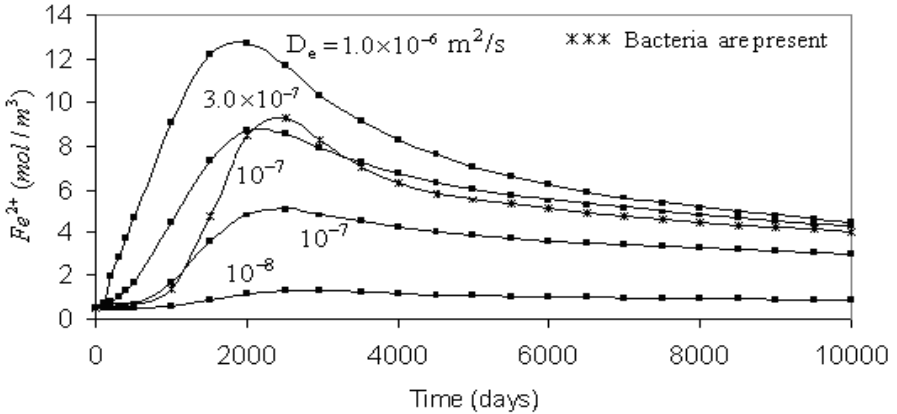

Figure 3. Ferrous iron concentration vs. time at the discharge boundary of the spoil profile for various effective diffusion coefficients

An increase in the effective diffusion coefficient also affected the ratio of ferrous iron to ferric iron. Figure 5 shows how variations in oxygen diffusion changed the Fe^{3+}/Fe^{2+} ratio predicted in the outflow boundary of the model. In this figure, a comparison was also made with the results obtained from the POLS model (dots), showing a close agreement. The increase in the effective diffusion coefficient increased the Fe^{3+}/Fe^{2+} ratio but it is not significant when chemical oxidation of ferrous iron is the only source of ferric iron.

Figure 6 shows sulphate concentrations as a function of time calculated at the outflow boundary of the model for different effective diffusion coefficients. Similar to ferrous iron concentration, the peak concentration of sulphate occurred at 2100 days. The maximum SO_4^{2-} concentration shifted from 52 to 75.2 mol/m^3 when the effective diffusion coefficient was changed from $1x10^{-8}$ to $1x10^{-6}$ m^2/s. This means that an increase in the diffusion coefficient caused more oxygen to be available for the oxidation reaction and consequently more sulphate was produced.

THE EFFECT OF IRON-OXIDISING BACTERIA

In the second simulation, the effective diffusion coefficient was assumed to be a constant equal to 1×10^{-7} m^2/s but the role of the iron-oxidising bacteria was taken into account. Oxygen did not diffuse more than 3 m (Figure 1). Bacterial activity was the main reason for this sharp reduction of oxygen concentration within the surface layers of the spoil profile, which consumed most of the oxygen over this part of the profile. No change was obtained for the pyrite oxidation rate where the interaction between H$^+$ and spoil was not considered. As illustrated in Figure 5, bacteria increased the Fe^{3+}/Fe^{2+} ratio about 100 times. An increase in the bacterial activity occurred when the solution pH was maintained between 2.5 to 3 by incorporating the spoil-H$^+$ interaction; therefore, the rate of pyrite oxidation is increased by ferric iron produced by the bacterially mediated reaction. As Figure 2 shows, the pyrite oxidation rate increased from 20% to 28% after 10000 days of the simulation due to this bacterial action. For spoil zones lacking oxygen, the ferric iron was the only oxidant available for pyrite oxidation.

Bacterial activity also has an effect on the concentration of ferrous iron and sulphate. For both ferrous iron (Figure 3) and sulphate (Figure 6), the peak or maximum concentration was slightly shifted to the lower layers. As Figure 3 shows, the ferrous iron concentration was increased from 5.03 mol/m^3 to 9.33 mol/m^3, and according to Figure 6, the sulphate concentration was increased from 60 mol/m^3 to 68.7 mol/m^3 at 2500 days after simulation. The main reason for these increases is that both oxygen and bacterially produced ferric iron participated in the pyrite oxidation reaction, and consequently in ferrous iron and sulphate generation.
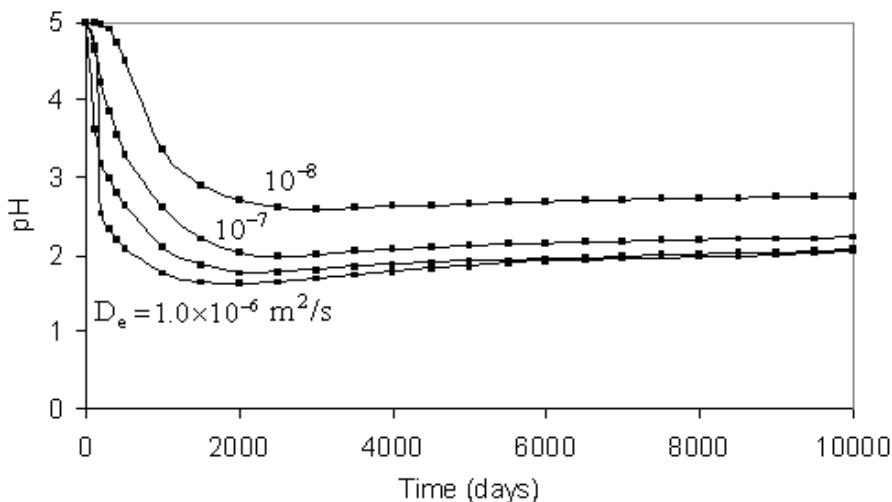

Figure 4. pH as a function of time at the discharge boundary of the spoil profile for various effective diffusion coefficients
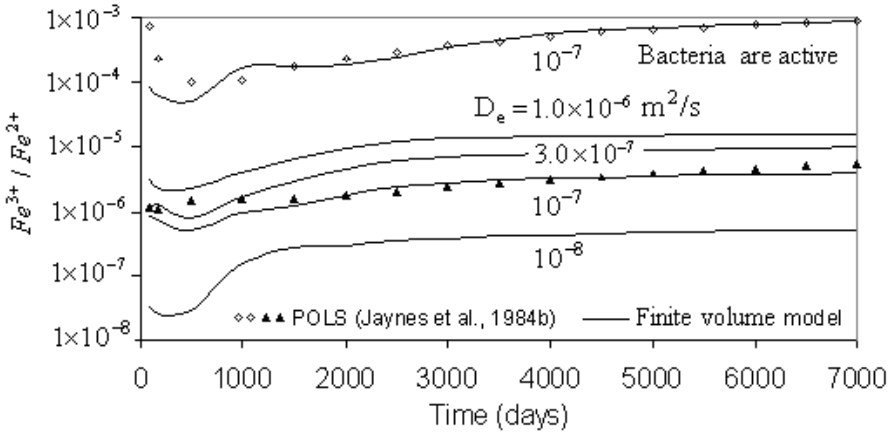
Figure 5. Predicted Fe^{3+}/Fe^{2+} ratio vs. time at the outlet boundary of the spoil profile for various effective diffusion coefficients
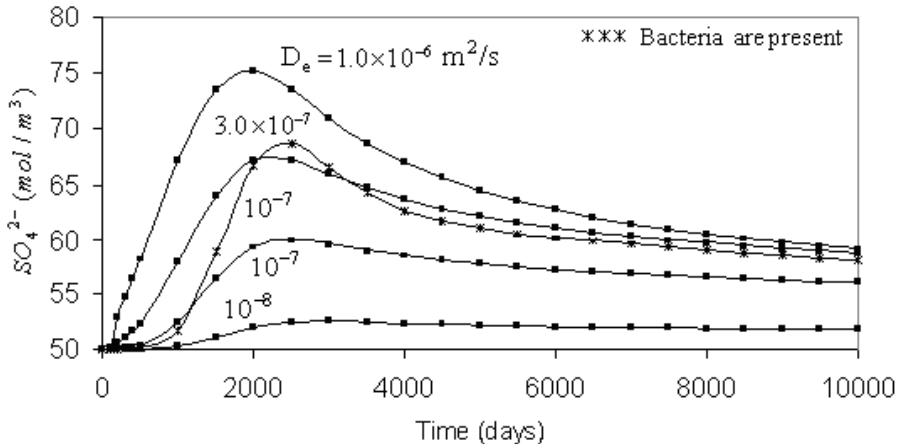

Figure 6. SO_4^{2-} concentration vs. time predicted at the outlet boundary of the spoil column for different effective diffusion coefficients

THE EFFECT OF PARTICLE SIZE

A simulation without the role of iron-oxidising bacteria was carried out to consider the sensitivity of the modelling quantities to the particle size of the surface mine spoil. Figures 7 through 10 show the simulation results for the fraction of pyrite consumed in the entire spoil column vs. time, ferrous iron concentration, solution pH, and sulphate concentration predicted at the model outlet boundary as a function of time shown for different spoil particle size. These results are for an effective diffusion coefficient of 1×10^{-7} m^2/s, a pyrite content of 0.25%, and a simulation time of 10000 days. The particle size varied from 6.0×10^{-3} m to 4.0×10^{-2} m. It is clear from Figure 7 that the smaller the particle size, the higher the fraction of pyrite oxidised.

It is obvious that when the particle size was reduced from 4.0×10^{-2} to 6.0×10^{-3} m, the pyrite oxidation rate increased from 13.9% to 32.6% after 10000 days.

It is clear from Figures 8 through 10 that the pyrite oxidation products, such as pH and the concentrations of Fe^{2+}, SO_4^{2-} are also sensitive to changes in the particle size of the spoil materials although this sensitivity is not very obvious in the solution pH. It has been illustrated that by reducing the particle size of the spoil materials, the ferrous iron (Figure 8) and sulphate concentration (Figure 10) are increased and the pH (Figure 9) is lowered.

THE EFFECT OF PYRITE CONTENT

The sensitivity of the model to changes in the pyrite content was also examined. Values of the pyrite content considered in this study ranged from 0.001 to 0.004. The modelling quantities are presented for the fraction of pyrite oxidised, the concentrations of ferrous iron, sulphate, and solution pH as a function of time predicted at the outflow boundary of the model in Figures 11 to 14. Figure 11 shows the fraction of pyrite oxidised plotted against time for different values of pyrite content. It is clear that the pyrite oxidation rate is also sensitive to variations in pyrite content. Lower pyrite content caused a higher oxidation rate. As depicted in Figure 11, when the pyrite content decreased from 0.0025 to 0.001, the pyrite oxidation rate increased from 20% to about 29% after 10000 days of pyrite oxidation. The oxidation rate was reduced from 20% to 16% when the pyrite content increased from 0.0025 to 0.004 at 10000 days.
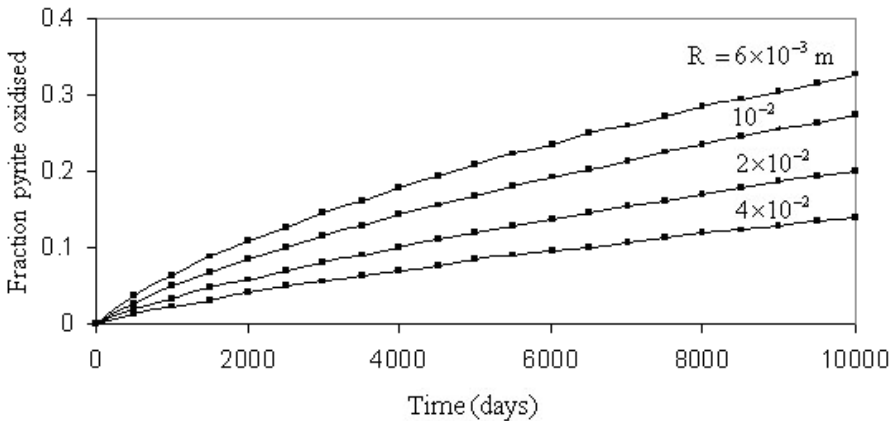

Figure 7. Pyrite fraction oxidised vs. time over entire spoil profile for different particle radii
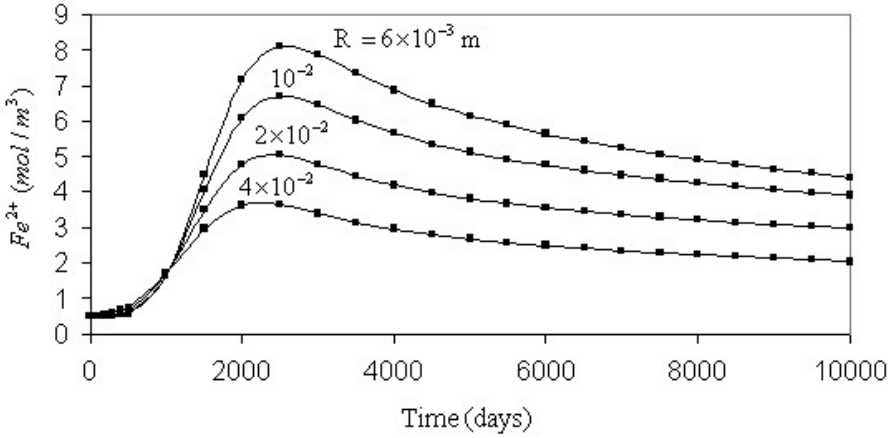
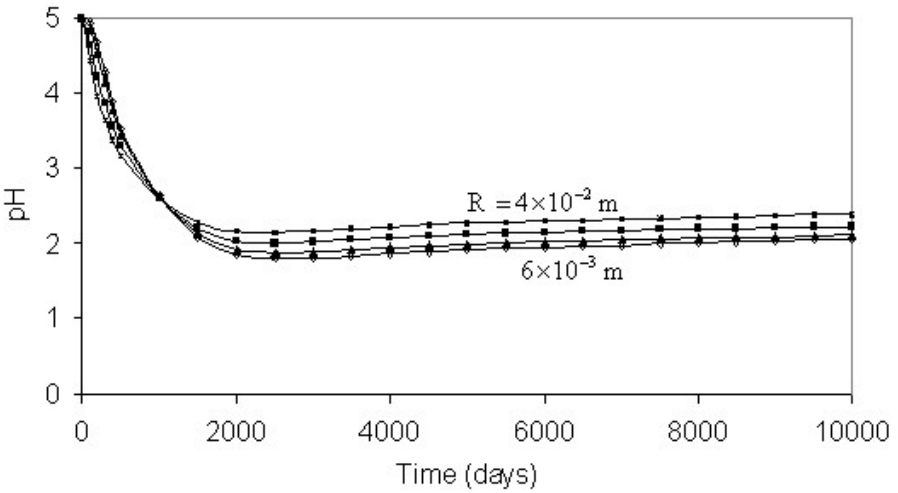*Figure 8. Fe^{2+} concentration vs. time at the outlet boundary of the spoil profile for different particle radii*

Figure 9. Solution pH vs. time at the discharge boundary of the spoil profile for various particle radii
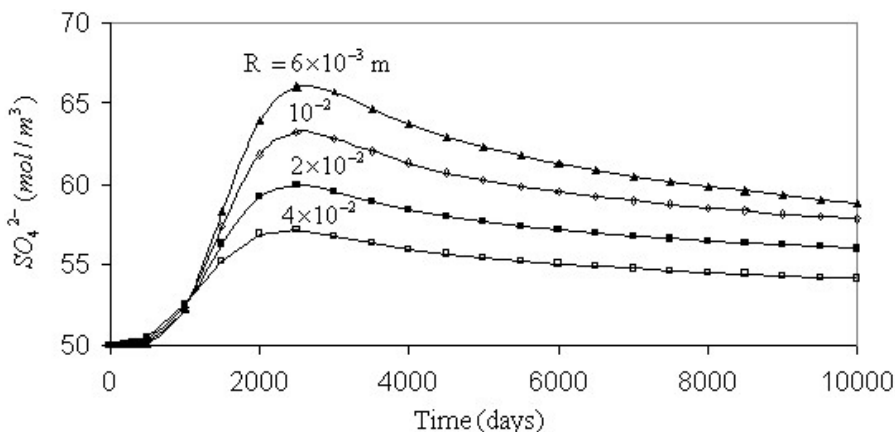
Figure 10. SO_4^{2-} concentration vs. time predicted at the outlet boundary of the spoil column for different particle radii
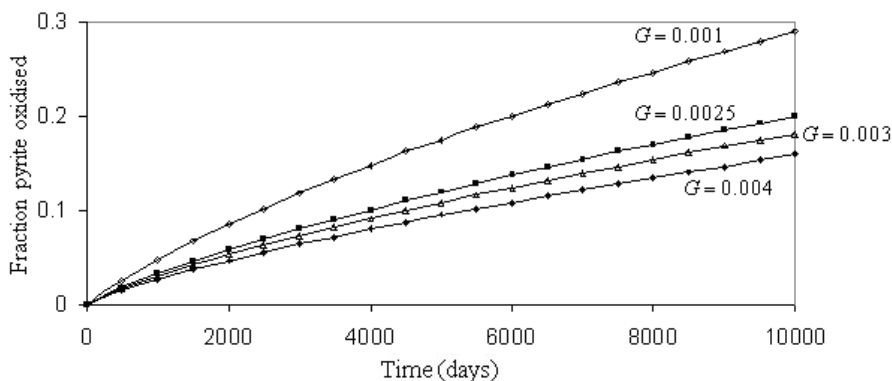

Figure 11. Pyrite fraction oxidised vs. time over the entire spoil profile for different pyrite contents

The oxidation products showed different behaviour when the pyrite content was changed. It is evident from Figures 12 through 14 that the lower the pyrite content, the lower the ferrous iron (Figure 12) and sulphate (Figure 14) production rate and the higher the solution pH (Figure 13). If the pyrite content within the spoil is small, then less oxygen will be required for the oxidation process and lower levels of contamination will be generated.

THE EFFECT OF SURFACE RECHARGE

The sensitivity of the modelling results to the surface recharge rate was also considered in this analysis. The simulation was performed in the absence of iron-oxidising bacteria. Although not shown, an increase in the recharge rate did not affect the pyrite oxidation rate but increased the recharge rate, changed the pH and the concentrations of Fe^{2+} and SO_4^{2-} predicted at the lower boundary of the spoil profile. According to Figure 15, when the surface recharge increased from 2×10^{-8} m/s to 5×10^{-8} m/s, the peak concentration of Fe^{2+} decreased

from 5 to 2.17 mol/m^3. It is clear from Figure 15 that the peak concentration was shifted from 2000-2500 days to 1000 days because the ferrous iron produced by the oxidation of pyrite is leached more quickly by the higher recharge rate, and therefore the peak concentration occurred at earlier times.

The pH was also affected by the changes made to the surface recharge rates. Figure 16 shows that increasing the recharge rate reduced the concentration of H$^+$; therefore, the pH increased. For a specific time of 10000 days, for example, the pH at the discharge boundary increased from 2.22 to 2.64.

Figure 17 shows sulphate concentration as a function of time for different values of surface recharges calculated at the outlet boundary of the model. Increasing the surface recharge from 2x10^{-8} m/s to 5x10^{-8} m/s considerably decreased the sulphate concentration; the peak concentration decreased from 60 to 54.2 mol/m^3.
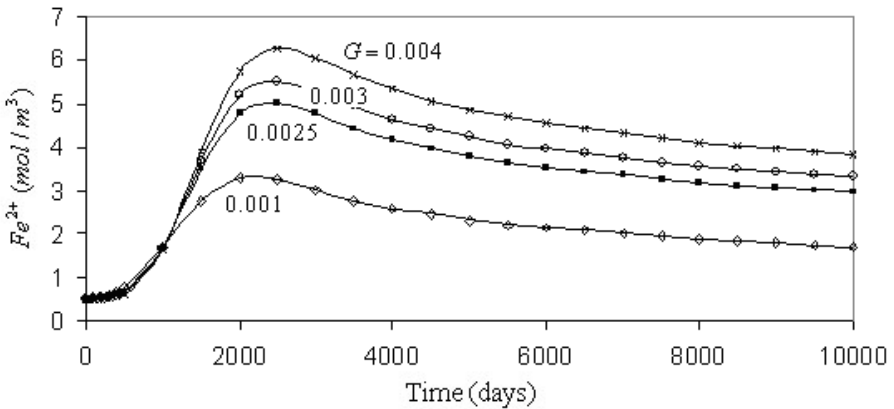

Figure 12. Fe^{2+} concentration vs. time at the outlet boundary of the profile for different pyrite contents of the spoil
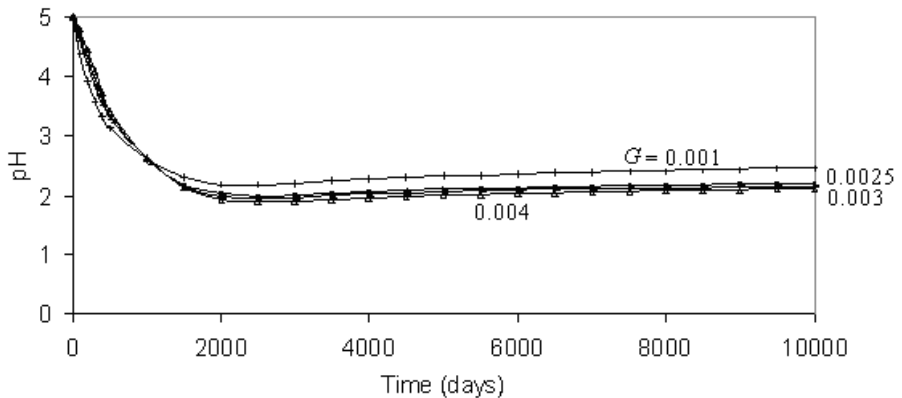

Figure 13. pH vs. time at the discharge boundary of the model for different values of pyrite content
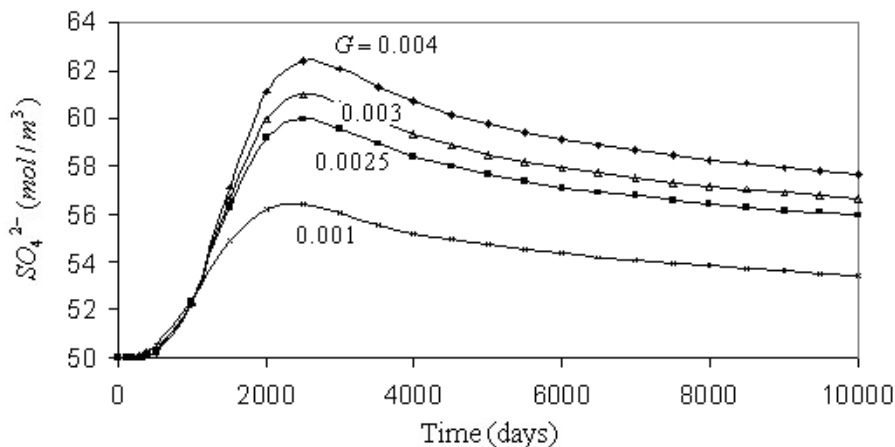
Figure 14. SO_4^{2-} concentration vs. time calculated at the outlet boundary of the spoil column for different pyrite contents
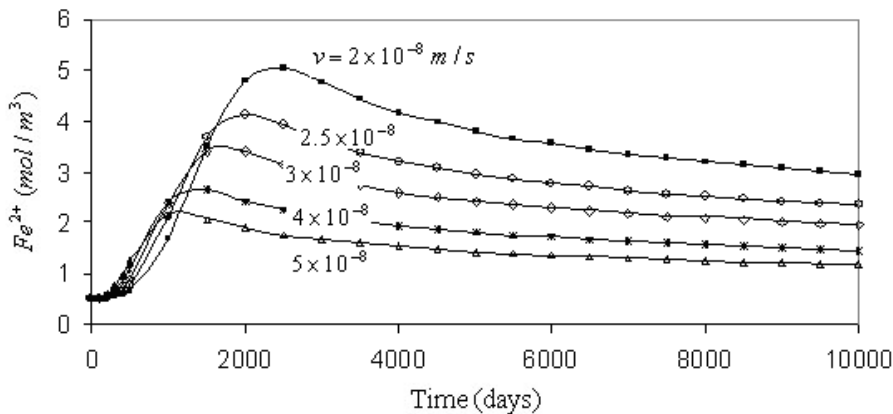

Figure 15. The predicted ferrous iron concentration at the outlet boundary of the model as a function of time for different surface recharges
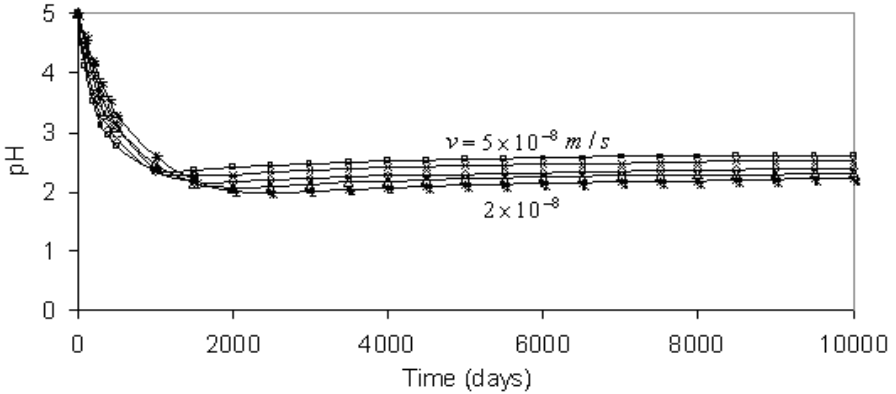
Figure 16. Solution pH vs. time at the discharge boundary of the spoil profile for different surface recharge values
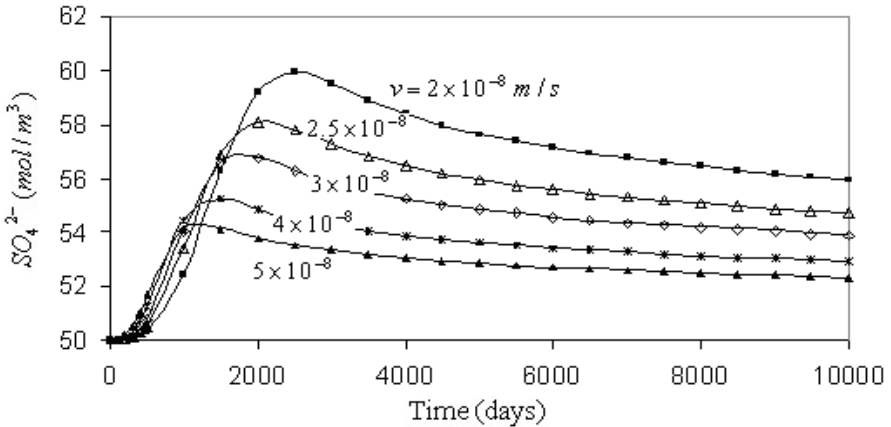

Figure 17. Sulphate concentration vs. time at the outlet boundary for different surface recharges values

CONCLUSIONS

In this investigation, the effects of changing parameters such as the effective diffusion coefficient for oxygen transport, the surface recharge rate, the particle radius, the pyrite content, and the role of iron-oxidising bacteria on the rate of pyrite oxidation were examined. The pyrite oxidation rate was increased by an increased effective diffusion coefficient for oxygen transport, decreased spoil particle size, and a decrease in pyrite content. The increase in the surface recharge did not affect the pyrite oxidation rate but changed the solution pH and the concentrations of Fe^{2+} and SO_4^{2-} predicted at the outlet boundary of spoil profile. Although iron-oxidising bacteria increased the ferric/ferrous ratio, the bacterially mediated oxidation of pyrite is highly dependent on pH. When the pH is maintained between 2.5 to 3.5, the bacterial oxidation of pyrite is enhanced. Subsequently, more Fe^{3+}, SO_4^{2-}, H^+, and Fe^{2+} is produced. Quantifying the effect of variations in model parameters is important when one wishes to reduce the pollutant production rate below an acceptable level in order to minimise the pollution load on the receiving environs of an open cut mine site.

REFERENCES

- *CHAM (2000) The PHOENICS On-Line Information System*, http://www.cham.co.uk/phoenics/d_polis/polis.htm
- Davis, G.B. (1983) Mathematical modelling of rate-limiting mechanisms of pyritic oxidation in overburden dumps. Ph.D. Thesis, University of Wollongong, Australia, 159p
- Doulati Ardejani, F., Singh, R.N. and Baafi, E.Y. (2002) A numerical finite volume model for prediction of pollution potential of open cut mine backfill. 6th Annual Environmental Engineering Research Event 2002 conference, Blackheath NSW, Australia
- Jaynes, D.B., Rogowski, A.S. and Pionke, H.B. (1984a) Acid mine drainage from reclaimed coal strip mines, 1, Model description. Water Resources Research, 20 (2), pp.233-242
- Jaynes, D.B., Rogowski, A.S. and Pionke, H.B. (1984b) Acid mine drainage from reclaimed coal strip mines, 2, Simulation results of model. Water Resources Research, 20 (2), pp.243-250
- Levenspiel, O. (1972) Chemical reaction engineering, John Wiley, New York, 578p
- Spalding, D.B. (1981) A general purpose computer program for multi-dimensional one- and two-phase flow. Mathematics and Computers in Simulation, 23(3), pp.267-276